High-Pressure Phase Equilibrium and Raman Spectroscopic Studies on the Nitrous Oxide Hydrate System

Takeshi Sugahara,* Akira Kawazoe, Keisuke Sugahara, and Kazunari Ohgaki

Division of Chemical Engineering, Department of Materials Engineering Science, Graduate School of Engineering Science, Osaka University, 1-3 Machikaneyama, Toyonaka, Osaka 560-8531, Japan

Thermodynamic stability boundaries of nitrous oxide (N_2O) hydrate and Raman spectra of the N_2O and host water molecules in the N_2O hydrate system were investigated in a temperature range of (275.20 to 298.19) K and a pressure range up to 305 MPa. Two three-phase coexisting curves of (hydrate + aqueous + gas) and (hydrate + aqueous + liquid N_2O) originate from the quadruple point of (hydrate + aqueous + liquid N_2O + gas) located at (285.15 ± 0.05) K and (4.2 ± 0.1) MPa. The phase behavior of the N_2O hydrate system is similar to that of the carbon dioxide (CO_2) hydrate system up to 100 MPa, while the stability boundaries of the N_2O hydrate system are shifted parallel to the (2 to 3) K higher temperature side than that of CO_2 hydrate. Raman peak splitting of the intramolecular vibration mode for the nitrous oxide molecule in the hydrate phase indicates the occupancy of the nitrous oxide molecule in both small and large cages of structure-I, and this observation is also corroborated by the pressure-induced Raman shift of the lattice mode.

Introduction

Gas hydrates are crystalline substances composed of the guest species and the cages which are constructed by the hydrogen-bonded water molecules. For about 200 years since the presence of gas hydrates was reported for the first time, many investigators have clarified the structure and thermodynamic stability boundary of gas hydrates with more than 120 guest species. Three common structures of gas hydrate are called structure-I (s-I), structure-II, and structure-H.[1] The s-I hydrate has two small cages (pentagonal dodecahedron, S-cages) and six middle cages (tetrakaidecahedron, M-cages) in the unit lattice. The familiar guest species for s-I are methane (CH_4, 0.44 nm), carbon dioxide (CO_2, 0.50 nm), ethane (C_2H_6, 0.53 nm), ethylene (C_2H_4, 0.55 nm) and so on. The value in parentheses represents the largest van der Waals diameter of each guest species. The Raman peak corresponding to the intramolecular C−H symmetric vibration mode of the CH_4 molecule in the CH_4 hydrate divides into doublets, and the peak intensity ratio corresponds to the cage-constituent ratio of s-I.[2,3] The C_2H_4 and C_2H_6 molecules, which are slightly larger than the void space of the S-cage, can oppressively occupy a part of the S-cage as the pressure increases, while they cannot occupy it in a low-pressure region.[4,5]

Nitrous oxide (N_2O, 0.51 nm) is one of the guest species forming a s-I hydrate. N_2O hydrate has a long history, and the existence of the N_2O hydrate was found by Villard in 1888.[6] After that, the thermodynamic stability boundary was reported in a lower-pressure region than the quadruple point (Q_2) of (hydrate + aqueous + liquid N_2O + gas).[7,8] Recently, Mohammadi and Richon[9] reported the phase relations of N_2O hydrate accompanied with CO_2 hydrate. N_2O has a similar molecular mass and similar critical constants to CO_2. The largest van der Waals diameter of N_2O (0.51 nm) is slightly larger than that of CO_2 (0.50 nm), and it is almost the same as the void size of the S-cage of s-I. In the CO_2 hydrate system, it had been believed that the CO_2 molecule cannot occupy the S-cage. However, the occupancy of CO_2 in both S- and M-cages is confirmed by the single-crystal X-ray diffraction[10] and FTIR[11] measurements. Therefore, it is very important to investigate the S-cage occupancy of N_2O as well as the phase equilibrium relation of the N_2O hydrate system.

In the present study, we have investigated the thermodynamic stability boundaries of the N_2O hydrate system in a temperature range of (275.20 to 298.19) K and a pressure range up to 305 MPa. In addition, the S-cage occupancy of the N_2O molecule and the pressure effect of the lattice mode of the N_2O hydrate have been briefly discussed from the Raman spectra of the intra- and intermolecular vibration modes.

Experimental Section

Research grade N_2O (purity is higher than 99.9 %) was purchased from Neriki Gas Co. Ltd. The distilled water was obtained from Yashima Pure Chemicals Co. Ltd. Both were used without further purification.

We used three types of high-pressure cells depending on the experimental pressures. The detail of the high-pressure cells is given elsewhere.[12] The equilibrium temperature was measured within a reproducibility of 0.02 K using a thermistor probe (Takara D-641) calibrated by a Pt resistance thermometer (25 Ω) defined by ITS-90. For pressure measurement, two different pressure gauges were used depending on the experimental pressure. Up to 75 MPa, a pressure gauge (Valcom VPRT) calibrated by a Ruska quartz Bourdon tube gauge was used with an estimated maximum uncertainty of 0.02 MPa. Over 75 MPa, a pressure transducer (NMB STD-5000K) and digital peak holder (NMB CSD-819) were used with an estimated maximum uncertainty of 2 MPa.

A desired amount of N_2O was introduced into the evacuated and cooled cell. A mixing magnet or a mixing ball in the cell

* Corresponding author. Telephone & Fax: +81-6-6850-6293. E-mail: sugahara@cheng.es.osaka-u.ac.jp.

10.1021/je900318u CCC: $40.75
Published on Web 05/19/2009

Table 1. Thermodynamic Stability Boundaries (Temperature *T*, Pressure *p*) of (Hydrate + Aqueous + Gas) and (Hydrate + Aqueous + Liquid N_2O) in the N_2O Hydrate System

T/K	*p*/MPa	*T*/K	*p*/MPa
hydrate + aqueous + gas		hydrate + aqueous + liquid N_2O	
275.20	1.20	285.80	10.56
276.25	1.32	286.34	16.12
277.01	1.45	286.35	16.25
277.71	1.58	286.43	17.01
278.39	1.70	286.51	17.75
279.18	1.87	286.74	20.36
279.94	2.04	287.03	23.58
280.73	2.26	287.30	26.72
281.51	2.48	287.35	27.31
282.39	2.79	287.45	28.28
282.79	2.94	287.60	30.21
283.19	3.12	288.03	35.35
283.47	3.24	288.38	39.57
283.67	3.34	288.79	44.89
283.87	3.41	289.11	49.21
284.06	3.54	289.31	52.38
284.37	3.76	289.52	55.43
284.58	3.91	289.71	58.10
284.76	3.99	289.98	61.67
284.97	4.15	291.85	91
		292.83	107
		296.26	202
		298.19	305

was vibrated from the outside for agitation. The contents were pressurized up to the desired pressure by a successive supply of water. After the formation of the N_2O hydrate, to establish the three-phase equilibrium state, the system temperature was gradually increased, and the contents were agitated intermittently. The phase behavior of the system was observed by the CCD camera through the sapphire window. To avoid a hysteresis effect, the stability boundary was measured with an annealing method.[13]

After the single crystal of N_2O hydrate was prepared on the stability boundary under a few pressure conditions, N_2O hydrate crystals were analyzed using a laser Raman microprobe spectrometer with a multichannel CCD detector (Jobin Yvon Ramanor T64000). The laser beam from the object lens irradiated the sample through the upper sapphire window. The backscatter of the opposite direction was taken in with the same lens. The argon ion laser beam of 514.5 nm and 100 mW was condensed to a 2 μm spot diameter. The spectral resolution was 0.7 cm^{-1}.

Results and Discussion

The thermodynamic stability boundaries of N_2O hydrate are listed in Table 1 and plotted in Figure 1. It is also compared with that of CO_2 hydrate.[12,14] The quadruple point Q_2 of (hydrate + aqueous + liquid N_2O + gas) phases, which was determined by the extrapolation of two three-phase coexistence curves, is located at (285.15 ± 0.05) K and (4.2 ± 0.1) MPa. The stability boundary in the lower-pressure range than the Q_2 agrees well with the literature.[6−9] The equilibrium temperature of N_2O hydrate is (2 to 3) K higher than that of CO_2 hydrate at the same pressure conditions below 100 MPa. Above 100 MPa, the temperature difference becomes gradually large, and it is 4.5 K at around 300 MPa.

From the slope of the equilibrium curve (d*p*/d*T*) in a lower-pressure region than Q_2, the overall enthalpy of hydrate dissociation ($\Delta_{hyd}H$) in the N_2O hydrate system was obtained by using the Clapeyron equation, the Soave−Redlich−Kwong equation of state,[15] and the ideal hydrate assumption of s-I. The details are given in the previous paper.[16] The average value of

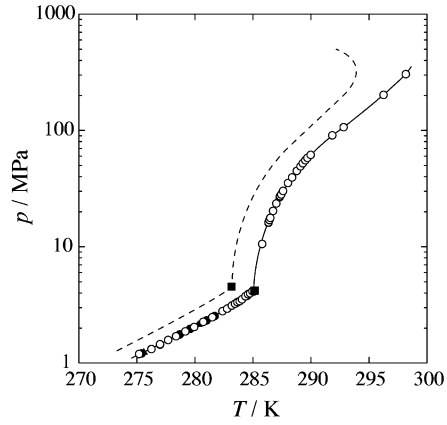

Figure 1. Thermodynamic phase boundaries of N_2O (open circles, present study; closed triangles, ref 7; closed circles, ref 9) and CO_2 (broken lines, refs 12 and 14) hydrate systems. The closed square symbols stand for the quadruple point Q_2 of hydrate + gas + liquid guest + aqueous phases.

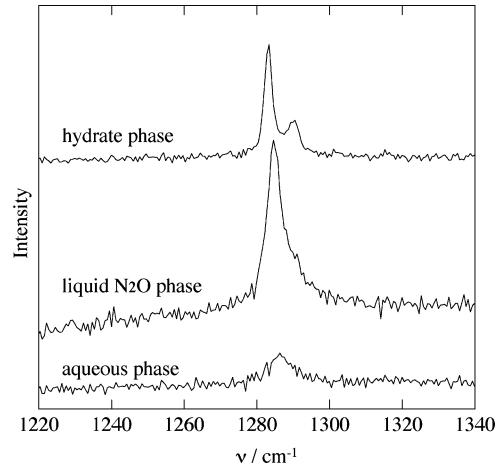

Figure 2. In situ Raman spectra corresponding to the N−O vibration mode of the N_2O molecule in N_2O hydrate and liquid N_2O and aqueous phases at 40 MPa and 288.43 K.

$\Delta_{hyd}H = (65 \pm 4)$ kJ·mol^{-1} shows good agreement with the literature value of 61.5 kJ·mol^{-1}.[17]

The N_2O molecule has three Raman-active vibration modes, N−O stretching vibration (around 1285 cm^{-1}), N−N stretching vibration (around 2230 cm^{-1}), and N−N−O bending vibration (around 580 cm^{-1}). The Raman peak of the N−O stretching vibration mode is the most intensive of the three Raman-active modes. Figure 2 shows the typical in situ Raman spectra corresponding to N−O vibration of the N_2O molecule in the hydrate, liquid N_2O, and aqueous phases on the thermodynamic stability boundary at 40 MPa and 288.43 K. The spectrum splits into a doublet (1283 cm^{-1} and 1290 cm^{-1}) in the N_2O hydrate phase, while a single peak is detected in both the liquid N_2O (1285 cm^{-1}) and aqueous (1287 cm^{-1}) phases. The shoulder at the higher wavenumber side of the Raman peak in the liquid N_2O phase is the overlap of the peak in the aqueous phase because small N_2O droplets are dispersed in the aqueous phase. The split of the Raman peak in the hydrate phase indicates that the N_2O molecules occupy both the S- and M-cages. The stronger peak (1283 cm^{-1}) corresponds to N_2O entrapped in the M-cages and the weaker one (1290 cm^{-1}) to the S-cages. This is also supported by the peak intensity ratio of N_2O in M-cage to S-cage, which is close to the cage-constituent ratio of the s-I hydrate. The Raman spectrum in the hydrate phase reveals that, even at 40 MPa, most of the S-cages are occupied by the N_2O molecules.

The Raman spectrum corresponding to the intermolecular O−O vibration (lattice mode) between water molecules depends on the hydrate structures, the pressure, and temperature conditions. On the thermodynamic stability boundary of hydrates, the pressure dependences of the O−O vibration energy are peculiar to the hydrate crystal structures for the s-I and s-II.[12,13,18−21] There are two types of pressure dependences in the s-I hydrate systems. One is strong pressure dependence (CH_4,[3] CO_2,[12] Xe,[19] and so on, type A). The other is very weak pressure dependence (ethane,[5] cyclopropane,[20] CF_4,[21] and so on, type B). The Raman peak of the O−O vibration in the N_2O hydrate crystal (not shown) is located at (204 ± 2) cm^{-1} (40 MPa and 288.23 K) and (210 ± 2) cm^{-1} (203 MPa and 296.39 K). The larger deviation than the original accuracy of the Raman spectrometer is caused by the low signal-to-noise ratio because it is more difficult than other hydrate systems to prepare a single crystal of N_2O hydrate along the thermodynamic stability boundary. Nevertheless, we can barely distinguish the pressure effect of the Raman shift. The pressure dependence of the O−O vibration energy in the N_2O hydrate is similar to that in the CO_2 hydrate system; that is, it belongs to the type A group of s-I. The stronger pressure dependence would indicate a higher shrinkage of the hydrogen-bonded cage or the larger free volume for the N_2O molecule.

Conclusion

We measured the thermodynamic stability boundaries of the N_2O hydrate system in a pressure range up to 305 MPa. The phase behavior of the N_2O hydrate system is qualitatively similar to that of the CO_2 hydrate system up to 100 MPa. One of the most important findings is that N_2O molecules can easily occupy both S- and M-cages of the structure-I hydrate. The peak intensity ratio of N_2O in the S-cage to the M-cage at 40 MPa and 288.15 K is close to the cage-constituent ratio of structure-I.

Acknowledgment

The authors are grateful to the Division of Chemical Engineering, Graduate School of Engineering Science, Osaka University, for the scientific support by "Gas-Hydrate Analyzing System (GHAS)".

Literature Cited

(1) Sloan, E. D.; Koh, C. A. *Clathrate Hydrates of Natural Gases*, 3rd ed.; CRC Press: Taylor & Francis Group, Boca Raton, 2007.
(2) Sum, A. K.; Burruss, R. C.; Sloan, E. D., Jr. Measurement of Clathrate Hydrates via Raman Spectroscopy. *J. Phys. Chem. B* **1997**, *101*, 7371–7377.
(3) Nakano, S.; Moritoki, M.; Ohgaki, K. High-Pressure Phase Equilibrium and Raman Microprobe Spectroscopic Studies on the Methane Hydrate System. *J. Chem. Eng. Data* **1999**, *44*, 254–257.
(4) Sugahara, T.; Morita, K.; Ohgaki, K. Stability Boundaries and Small Hydrate-Cage Occupancy of Ethylene Hydrate System. *Chem. Eng. Sci.* **2000**, *55*, 6015–6020.
(5) Morita, K.; Nakano, S.; Ohgaki, K. Structure and Stability of Ethane Hydrate Crystal. *Fluid Phase Equilib.* **2000**, *169*, 167–175.
(6) Villard, M. Sur Quelques Nouveaux Hydrates de Gaz. *Compt. Rend.* **1888**, *106*, 1602–1603.
(7) Villard, M. P. Etude Experimentale des Hydrates de Gaz. *Ann. Chim. Phys.* **1897**, *11*, 289–394.
(8) von Tammann, G.; Krige, G. J. R. Die Gleichgewichtsdrucke von Gashydraten. *Z. Anorg. Allg. Chem.* **1925**, *146*, 179–195.
(9) Mohammadi, A. H.; Richon, D. Equilibrium Data of Nitrous Oxide and Carbon Dioxide Clathrate Hydrates. *J. Chem. Eng. Data* **2009**, *54*, 279–281.
(10) Udachin, K. A.; Ratcliffe, C. I.; Ripmeester, J. A. Structure, Composition, and Thermal Expansion of CO_2 Hydrate from Single Crystal X-ray Diffraction Measurements. *J. Phys. Chem. B* **2001**, *105*, 4200–4204.
(11) Prasad, P. S. R.; Prasad, K. S.; Thakur, N. K. FTIR Signatures of Type-II Clathrates of Carbon Dioxide in Natural Quartz Veins. *Curr. Sci.* **2006**, *90*, 1544–1547.
(12) Nakano, S.; Moritoki, M.; Ohgaki, K. High-Pressure Phase Equilibrium and Raman Microprobe Spectroscopic Studies on the CO_2 Hydrate System. *J. Chem. Eng. Data* **1998**, *43*, 807–810.
(13) Sugahara, K.; Kaneko, R.; Sasatani, A.; Sugahara, T.; Ohgaki, K. Thermodynamic and Raman Spectroscopic Studies of Ar Hydrate System. *Open Thermodyn. J.* **2008**, *2*, 95–99.
(14) Ohgaki, K.; Hamanaka, T. Phase-Behavior of CO_2 Hydrate-Liquid CO_2-H_2O System at High Pressure. *Kagaku Kogaku Ronbunshu* **1995**, *21*, 800–803.
(15) Soave, G. Equilibrium Constants from a Modified Redlich-Kwong Equation of State. *Chem. Eng. Sci.* **1972**, *27*, 1197–1203.
(16) Sugahara, T.; Ohgaki, K. Border Gas Hydrate System Having Quadruple Point of Hydrate + Two Liquids + Gas Phases. *J. Chem. Eng. Jpn.* **2000**, *33*, 174–176.
(17) von Stackelberg, M.; Meinhold, W. Feste GasHydrate III: Mischhydrate. *Z. Elektrochem.* **1954**, *58*, 40–45.
(18) Sugahara, K.; Tanaka, Y.; Sugahara, T.; Ohgaki, K. Thermodynamic Stability and Structure of Nitrogen Hydrate Crystal. *J. Supramol. Chem.* **2002**, *2*, 365–368.
(19) Sugahara, K.; Sugahara, T.; Ohgaki, K. Thermodynamic and Raman Spectroscopic Studies of Xe and Kr Hydrates. *J. Chem. Eng. Data* **2005**, *50*, 274–277.
(20) Suzuki, M.; Tanaka, Y.; Sugahara, T.; Ohgaki, K. Pressure Dependence of Small-Cage Occupancy in the Cyclopropane Hydrate System. *Chem. Eng. Sci.* **2001**, *56*, 2063–2067.
(21) Sugahara, K.; Yoshida, M.; Sugahara, T.; Ohgaki, K. High-Pressure Phase Behavior and Cage Occupancy for the CF_4 Hydrate System. *J. Chem. Eng. Data* **2004**, *49*, 326–329.

Received for review March 31, 2009. Accepted April 30, 2009.

JE900318U